their maximum extensibility limit very rapidly.

Acknowledgment. This work was supported in part by Grant 0933/82 from the CAICYT (Spain). T.V. is grateful to a NATO postdoctoral research fellowship (while at Cambridge) arranged by the German Academic Exchange Service (DAAD).

Appendix

Substituting eq 6 in eq 19, we get

$$I(\alpha,R) = I_1(\alpha,R) + I_2(\alpha,R) \quad \text{(A1)}$$

where

$$I_1(\alpha,R) = -a_{00}\alpha R^2 \int_0^\pi \cos^2\theta(2 - \alpha^{-3}\tan^2\theta)\sin\theta\,d\theta \quad \text{(A2)}$$

and

$$I_2(\alpha,R) = -2b_{00}{}^2\alpha^3 R^4 \int_0^\pi \cos^4\theta(1 + \alpha^{-3}\tan^2\theta) \times (2 - \alpha^{-3}\tan^2\theta)\sin\theta\,d\theta \quad \text{(A3)}$$

and, through straightforward simplifications, we get

$$I_1(\alpha,R) = -a_{00}R^2\left[2\alpha\int_0^\pi \cos^2\theta\sin\theta\,d\theta - \alpha^{-2}\int_0^\pi \sin^3\theta\,d\theta\right] \quad \text{(A4)}$$

together with

$$I_2(\alpha,R) = -2b_{00}R^4\left[2\alpha^3\int_0^\pi \cos^4\theta\sin\theta\,d\theta + \int_0^\pi \cos^2\theta\sin\theta\,d\theta - \alpha^{-3}\int_0^\pi \sin^5\theta\,d\theta\right] \quad \text{(A5)}$$

The involved integrals are simply solved so that the results for I_1 and I_2 are written as the first and second terms on the right side of eq 20.

References and Notes

(1) Llorente, M. A.; Rubio, A. M.; Freire, J. J. *Macromolecules* **1984**, *17*, 2307.
(2) Mark, J. E.; Curro, J. G. *J. Chem. Phys.* **1983**, *79*, 5705.
(3) Curro, J. G.; Mark, J. E. *J. Chem. Phys.* **1984**, *80*, 4521.
(4) Andrady, A. L.; Llorente, M. A.; Mark, J. E. *J. Chem. Phys.* **1980**, *72*, 2282.
(5) Llorente, M. A.; Andrady, A. L.; Mark, J. E. *J. Polym. Sci., Polym. Phys. Ed.* **1981**, *19*, 621.
(6) Edwards, S. F. In "Polymer Networks"; Chromff, A., Newman, S., Ed.; Plenum Press: New York, 1971.
(7) Deam, R. I.; Edwards, S. F. *Philos. Trans. R. Soc. London* **1976**, *11*, 317.
(8) Freire, J.; Fixman, M. *J. Chem. Phys.* **1978**, *69*, 634.
(9) Freire, J. J.; Rodrigo, M. M. *J. Chem. Phys.* **1980**, *72*, 6376.
(10) Fixman, M.; Skolnick, J. *J. Chem. Phys.* **1976**, *65*, 1700.
(11) Treolar, L. R. G. "The Physics of Rubber Elasticity", 3rd ed.; Clarendon Press: Oxford, 1975.
(12) Mooney, M. *J. Appl. Phys.* **1948**, *19*, 434. Rivlin, R. S. *Philos. Trans. R. Soc. London, Ser. A* **1948**, *241*, 379.
(13) Llorente, M. A.; Mark, J. E. *J. Chem. Phys.* **1979**, *71*, 682.

Transient Viscoelastic Properties of Linear Polymer Solutions

Yoshiaki Takahashi,* Yoshinobu Isono,† Ichiro Noda, and Mitsuru Nagasawa

Department of Synthetic Chemistry, Nagoya University, Chikusa-ku, Nagoya 464, Japan.
Received July 10, 1985

ABSTRACT: Shear and normal stress developments after stepwise increases of shear rate from a steady shear rate $\dot{\gamma}_1$ to a higher one $\dot{\gamma}_2$ were observed with a Weissenberg rheogoniometer Type R-17 in linear polystyrene solutions. The initial parts of the stress-development curves at different $\dot{\gamma}_2$ compose a single line if $\dot{\gamma}_1$ is kept constant, and the initial slope becomes lower with increasing $\dot{\gamma}_1$. It was concluded that the original quasi-network structure of polymer solutions remains unchanged until a certain critical strain is accumulated in the solution. The difference in the initial slope at different $\dot{\gamma}_1$ may be caused by a change in the effective entanglement density with $\dot{\gamma}$. It is also pointed out that the additivity of responses in viscoelastic behavior of polymer solutions does not hold in nonlinear regions.

Introduction

In concentrated solutions and melts of linear polymers the polymer molecules are entangled with each other, forming a quasi-network structure. The entanglements may be dissolved and re-formed continuously, and the structure of the solution may be represented by the equilibrium entanglement density. The effective entanglement density is changed by external stimuli given to the polymer solution, such as shear rate.[1-3] It was pointed out in previous papers[4,5] that the structure cannot be changed at the instant when an external stimulus is given to the solution, but changes with a time lag. It is as if the quasi-network is ruptured when a certain strain has accumulated in the solution. This speculation was experimentally supported by observing the stress developments in a polymer solution when a steady shear flow is instantly given to the solution. The initial slopes of the transient viscosity vs. time plots at various shear rates agreed with that at the limit of zero shear rate, independent of shear rate.[4-7]

Under steady shear flow, polymer solutions have a quasi-network structure characterized by an effective density of entanglements, which decreases with increasing shear rate. It may, therefore, be reasonable to predict that the steady structure of polymer solutions at $\dot{\gamma}_1$ would not be changed to that at $\dot{\gamma}_2$ at the instant when the shear rate is instantly changed from $\dot{\gamma}_1$ to a higher value $\dot{\gamma}_2$ but that the rupture of the original structure would occur with a certain time lag. An aim of this work is to test the idea of the network-rupture model by observing stress development after a stepwise increase of shear rate from a value $\dot{\gamma}_1$ to a higher value $\dot{\gamma}_2$.

Moreover, the viscoelastic properties of polymer solutions and melts are phenomenologically described by various types of constitutive equations, usually by those of the so-called single-integral type with a memory function $\mu(t - t')$ or an aftereffect function $\phi(t - t')$, where t and t' are the present and past time, respectively.[8,9] These

† Present address: Department of Material Science and Technology, Technological University of Nagaoka, Nagaoka 949-54, Japan

0024-9297/86/2219-1217$01.50/0

constitutive equations agree with each other and account satisfactorily for experimental data in the linear region, although the assumption of negligible secondary normal stress difference is, strictly speaking, open to discussion. If we employ the aftereffect function $\phi(t - t')$ for convenience, the constitutive equation is

$$\mathbf{P}(t) = -p\mathbf{1} - \int_{-\infty}^{t} \phi(t - t') \left\{ \frac{\mathrm{d}}{\mathrm{d}t'} \boldsymbol{\lambda}(t,t') \right\} \mathrm{d}t' \qquad (1)$$

where $\mathbf{P}$ is the total stress tensor, p is the scalar pressure, and $\boldsymbol{\lambda}(t,t')$ is the Finger relative strain tensor.

Extension of these single-integral equations to nonlinear phenomena by modifying $\mu(t - t')$ or $\phi(t - t')$ as a function of strain or strain rate has also been attempted by many workers.[9,10] In this kind of extension, however, it should be noted that the additivity of responses to external stimuli is assumed even in nonlinear regions. Although experimental tests of such nonlinear constitutive equations are not the aim of this paper, the observation of stress development after a stepwise increase of shear rate from $\dot{\gamma}_1$ to $\dot{\gamma}_2$ may be useful for examining the assumption of additivity.

Theory

Let us assume that eq 1 may be extended to non-Newtonian flow if we express the aftereffect function as a function of shear rate $\dot{\gamma}$ as $\phi(t - t'|\dot{\gamma})$. The shear stress under a steady shear flow $P_{12}(\dot{\gamma})$ or the steady shear viscosity $\eta(\dot{\gamma})$ is then given by

$$\begin{aligned} P_{12}(\dot{\gamma}) &\equiv \dot{\gamma}\eta(\dot{\gamma}) \\ &= \dot{\gamma} \int_{-\infty}^{t} \phi(t - t'|\dot{\gamma})\, \mathrm{d}t' \end{aligned} \qquad (2)$$

Further, the transient shear stress $P_{12}^{\mathrm{d}}(t|\dot{\gamma})$ developed when a steady shear flow with shear rate $\dot{\gamma}$ is instantly given to a resting solution at $t = 0$, or the transient viscosity $\eta^{\mathrm{d}}(t|\dot{\gamma})$, is given by

$$\begin{aligned} P_{12}^{\mathrm{d}}(t|\dot{\gamma}) &\equiv \dot{\gamma}\eta^{\mathrm{d}}(t|\dot{\gamma}) \\ &= \dot{\gamma} \int_{0}^{t} \phi(t - t'|\dot{\gamma})\, \mathrm{d}t' \end{aligned} \qquad (3)$$

Moreover, the transient shear stress development $P_{12}^{\mathrm{d}}(t|\dot{\gamma}_1 \rightarrow \dot{\gamma}_2)$ observed when the shear rate is instantly changed from $\dot{\gamma}_1$ to a higher value $\dot{\gamma}_2$ at $t = 0$ should be

$$\begin{aligned} P_{12}^{\mathrm{d}}(t|\dot{\gamma}_1 \rightarrow \dot{\gamma}_2) &\equiv \dot{\gamma}_1 \int_{-\infty}^{0} \phi(t - t'|\dot{\gamma}_1)\, \mathrm{d}t' + \\ &\qquad \dot{\gamma}_2 \int_{0}^{t} \phi(t - t'|\dot{\gamma}_2)\, \mathrm{d}t' \\ &= \dot{\gamma}_1 \int_{-\infty}^{t} \phi(t - t'|\dot{\gamma}_1)\, \mathrm{d}t' + \dot{\gamma}_2 \int_{0}^{t} \phi(t - \\ &\qquad t'|\dot{\gamma}_2)\, \mathrm{d}t' - \gamma_1 \int_{0}^{t} \phi(t - t'|\dot{\gamma}_1)\, \mathrm{d}t' \\ &= P_{12}(\dot{\gamma}_1) + P_{12}^{\mathrm{d}}(t|\dot{\gamma}_2) - P_{12}^{\mathrm{d}}(t|\dot{\gamma}_1) \end{aligned} \qquad (4)$$

Here we have employed an aftereffect function of the rate-dependent type $\phi(t - t'|\dot{\gamma})$ for convenience. In analyzing the nonlinear behavior of viscoelasticity, however, it is often assumed that the aftereffect function is a function of the relative strain $\gamma(t,t')$ or some other parameters. In any case, the relationship (4) should hold whenever it is assumed that the effects of two stimuli $\dot{\gamma}_1$ and $\dot{\gamma}_2$ are additive, as implied in eq 1.

If we define the excess transient viscosity $\eta^{\mathrm{e}}(t|\dot{\gamma}_1 \rightarrow \dot{\gamma}_2)$ by

$$\eta^{\mathrm{e}}(t|\dot{\gamma}_1 \rightarrow \dot{\gamma}_2) \equiv \{P_{12}^{\mathrm{d}}(t|\dot{\gamma}_1 \rightarrow \dot{\gamma}_2) - P_{12}(\dot{\gamma}_1)\}/(\dot{\gamma}_2 - \dot{\gamma}_1) \qquad (5)$$

eq 4 becomes

$$\eta^{\mathrm{e}}(t|\dot{\gamma}_1 \rightarrow \dot{\gamma}_2) = \{P_{12}^{\mathrm{d}}(t|\dot{\gamma}_2) - P_{12}^{\mathrm{d}}(t|\dot{\gamma}_1)\}/(\dot{\gamma}_2 - \dot{\gamma}_1) \qquad (6)$$

Likewise, if the excess transient normal stress coefficient $\Psi_{12}^{\mathrm{e}}(t|\dot{\gamma}_1 \rightarrow \dot{\gamma}_2)$ is defined by

$$\begin{aligned} \Psi_{12}^{\mathrm{e}}(t|\dot{\gamma}_1 \rightarrow \dot{\gamma}_2) \equiv \{&(P_{11} - P_{22})^{\mathrm{d}}(t|\dot{\gamma}_1 \rightarrow \dot{\gamma}_2) \\ &- (P_{11} - P_{22})(\dot{\gamma}_1)\}/(\dot{\gamma}_2^2 - \dot{\gamma}_1^2) \end{aligned} \qquad (7)$$

it should be true that

$$\begin{aligned} &\Psi_{12}^{\mathrm{e}}(t|\dot{\gamma}_1 \rightarrow \dot{\gamma}_2) = \\ &\quad \{(P_{11} - P_{22})^{\mathrm{d}}(t|\dot{\gamma}_2) - (P_{11} - P_{22})^{\mathrm{d}}(t|\dot{\gamma}_1)\}/(\dot{\gamma}_2^2 - \dot{\gamma}_1^2) \end{aligned} \qquad (8)$$

If both $\dot{\gamma}_1$ and $\dot{\gamma}_2$ are sufficiently low, that is, in the linear region, both $\phi(t - t'|\dot{\gamma}_1)$ and $\phi(t - t'|\dot{\gamma}_2)$ are equal to $\phi(t - t'|0)$ $(\equiv\phi(t - t'))$ and, hence, eq 6 and 8 respectively become

$$\eta^{\mathrm{e}}(t|\dot{\gamma}_1 \rightarrow \dot{\gamma}_2) = \int_{0}^{t} \phi(t - t'|0)\, \mathrm{d}t' = \eta^{\mathrm{d}}(t|0) \qquad (9)$$

$$\Psi_{12}^{\mathrm{e}}(t|\dot{\gamma}_1 \rightarrow \dot{\gamma}_2) = 2\int_{0}^{t} \phi(t - t'|0)t'\, \mathrm{d}t' = \Psi_{12}^{\mathrm{d}}(t|0) \qquad (10)$$

where $\eta^{\mathrm{d}}(t|0)$ and $\Psi_{12}^{\mathrm{d}}(t|0)$ are the transient viscosity and transient normal stress coefficient at the limit of zero shear rate, respectively. Thus, both $\eta^{\mathrm{e}}(t|\dot{\gamma}_1 \rightarrow \dot{\gamma}_2)$ and $\Psi_{12}^{\mathrm{e}}(t|\dot{\gamma}_1 \rightarrow \dot{\gamma}_2)$ are independent of $\dot{\gamma}$ in the linear region.

In nonlinear regions, that is, if $\dot{\gamma}_1$ and/or $\dot{\gamma}_2$ are high, eq 6 and 8 cannot be expressed by such simple relationships as eq 9 and 10. The validity of eq 6 and 8 should be examined by inserting the transient stress data directly into those equations. However, we speculated in the Introduction that the structure of the solution would transform from state $\dot{\gamma}_1$ to that of $\dot{\gamma}_2$ with a time lag t_c. If this speculation is correct, the aftereffect function would remain unchanged in a time range $t \leq t_c$. We would then have

$$\begin{aligned} P_{12}^{\mathrm{d}}(t|\dot{\gamma}_1 \rightarrow \dot{\gamma}_2) = \dot{\gamma}_1 &\int_{-\infty}^{t} \phi(t - t'|\dot{\gamma}_1)\, \mathrm{d}t' + \\ (\dot{\gamma}_2 - \dot{\gamma}_1) &\int_{0}^{t} \phi(t - t'|\dot{\gamma}_1)\, \mathrm{d}t' \qquad \text{for } t \leq t_c \end{aligned} \qquad (11)$$

That is

$$\eta^{\mathrm{e}}(t|\dot{\gamma}_1 \rightarrow \dot{\gamma}_2) = \int_{0}^{t} \phi(t - t'|\dot{\gamma}_1)\, \mathrm{d}t' \qquad (12)$$

Likewise

$$\Psi_{12}^{\mathrm{e}}(t|\dot{\gamma}_1 \rightarrow \dot{\gamma}_2) = 2\int_{0}^{t} \phi(t - t'|\dot{\gamma}_1)t'\, \mathrm{d}t' \qquad (13)$$

Therefore, the initial growth of $\eta^{\mathrm{e}}(t|\dot{\gamma}_1 \rightarrow \dot{\gamma}_2)$ and $\Psi_{12}^{\mathrm{e}}(t|\dot{\gamma}_1 \rightarrow \dot{\gamma}_2)$ would compose a single line independent of $\dot{\gamma}_2$ if $\dot{\gamma}_1$ is kept constant. However, the slope would vary if $\dot{\gamma}_1$ is varied.

Beyond t_c, the aftereffect function would gradually transfer from $\phi(t - t'|\dot{\gamma}_1)$ to $\phi(t - t'|\dot{\gamma}_2)$ while the stresses are developed in the solution, causing a peak in the stress-development curves.

Experimental Methods

Linear polystyrene F-288 (Toyo Soda Manufacturing Co. Ltd.), with a weight-average molecular weight of 2.89×10^6 and a narrow molecular weight distribution, was dissolved in α-chloronaphthalene (α-CN) at 13.8, 12.9, and 10.5 g/dL. The zero-shear viscosity η^0 and steady-state compliance J_e of the solutions at these concentrations are listed in Table I. The purification methods and physical properties of α-CN have already been reported.[1]

The stress development in the stepwise increases of shear rate from the rest state and also from steady states at various shear

Table I
Steady Flow Viscosity and Compliance at Zero Shear Rate

C, g/dL	η^0, P	J_e, cm^2/dyn
13.8	1.34×10^4	
12.9	1.03×10^4	1.02×10^{-4}
10.5	2.79×10^3	1.88×10^{-4}

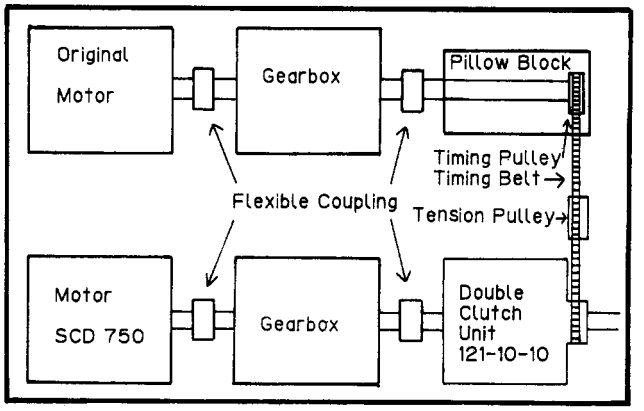

Figure 1. Schematic diagram of the modified drive unit of the Type R-17 Weissenberg rheogoniometer.

rates to higher shear rates were observed with Weissenberg rheogoniometer Type R-17 (Sangamo Controls Ltd.), equipped with a gap-servo system. The drive unit of the R-17 was modified to actualize the stepwise change of shear rates. A schematic diagram of the modified drive unit is shown in Figure 1. In additiion to the original motor and gearboxes of the R-17, a new motor (Type SCD 750) and a double-clutch unit (Type 121-10-10, Miki Pulley Co. Ltd.) are mounted on an antivibration mounting. Two electromagnetic clutches are connected to one shaft in the double-clutch unit. One motor and gearbox set is directly connected with the double-clutch unit by a flexible coupling, while the other set is connected by a timing belt and a timing pulley. Switching between two drives is controlled by a Type BEQ-10 control panel (Miki Pulley Co. Ltd.). The switching time is 40 ms at the maximum load. In the present experimental range, changes of shear rate by this modified drive unit may be regarded as stepwise changes. A cone with a 4° angle and 5-cm diameter was used. The temperature was kept at 50.0 ± 0.1 °C. The observed values were continuously recorded on an electromagnetic recorder. The reliability of measurements with Sangamo's Type R-17 was confirmed as reported previously.[11-13]

Results and Discussion

Shear and normal stress developments in polystyrene solutions were observed after stepwise increases of steady shear rate from various values of shear rate ($\dot{\gamma}_1$) to a constant shear rate ($\dot{\gamma}_2$) and also from a constant shear rate ($\dot{\gamma}_1$) to various shear rates ($\dot{\gamma}_2$) ($P_{12}{}^d(t|\dot{\gamma}_1 \rightarrow \dot{\gamma}_2)$ and $(P_{11} - P_{22})^d(t|\dot{\gamma}_1 \rightarrow \dot{\gamma}_2)$), in addition to those from rest to various values of shear rate ($\dot{\gamma}$) ($P_{12}{}^d(t|\dot{\gamma})$ and $(P_{11} - P_{22})^d(t|\dot{\gamma})$), which were already reported for poly(α-methylstyrene) solutions in previous papers.[4,5,12]

The transient viscosity $\eta^d(t|\dot{\gamma})$ is independent of $\dot{\gamma}$ if $\dot{\gamma}$ is low enough and composes a single line, as reported in previous papers. The $\eta^d(t|0)$ data in the linear region are shown by a solid line in Figure 2. The excess transient viscosity $\eta^e(t|\dot{\gamma}_1 \rightarrow \dot{\gamma}_2)$ in the region of sufficiently low $\dot{\gamma}$ is calculated from eq 5 by using the experimental $P_{12}{}^d(t|\dot{\gamma}_1 \rightarrow \dot{\gamma}_2)$ data and steady shear stress at $\dot{\gamma}_1$, $P_{12}(\dot{\gamma}_1)$, and is shown by circles in Figure 2. It is clear that the relationship in eq 9, i.e., eq 6, is experimentally confirmed if shear rates are low enough. This agreement may also be regarded as confirmation of the present experimental procedure. The normal stress development could not be observed with high accuracy in this region.

Examples of shear stress developments after stepwise increases of shear rate from various $\dot{\gamma}_1$ to a constant $\dot{\gamma}_2$ in nonlinear regions are shown by circles in Figure 3. The values of steady shear stress at $\dot{\gamma}_1$, $P_{12}(\dot{\gamma}_1)$, should be shown on the ordinate at $t = 0$ but are given in the figure caption. The stress development in the experiment from rest to the

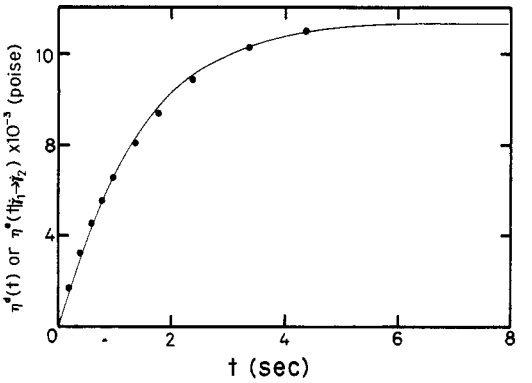

Figure 2. Experimental shear stress development function in the linear region. The solid line denotes the master curve of transient viscosity (η^d) observed after the onset of steady shear flow. Circles denote excess transient viscosity (η^e) observed when the shear rate is changed from $\dot{\gamma}_1 = 0.0216$ s^{-1} to $\dot{\gamma}_2 = 0.0500$ s^{-1}. Sample is an α-CN solution of F-288 (13.8 g/dL).

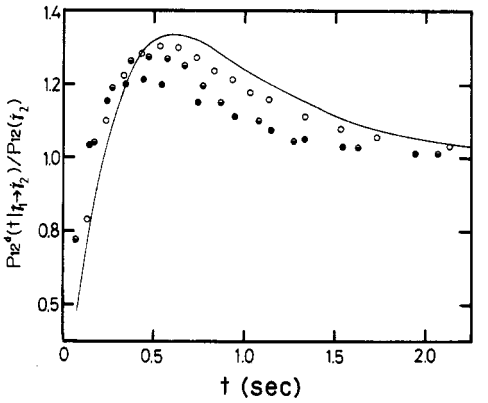

Figure 3. Experimental shear stress development in the stepwise increase of shear rate from various $\dot{\gamma}_1$ to a constant $\dot{\gamma}_2$ (3.96 s^{-1}) for the same sample as in Figure 1. The solid line denotes the data from rest. (○), (●), and (⊖) denote the data from $\dot{\gamma}_1 = 0.216$, 0.544, and 1.08 s^{-1}, respectively. The steady shear stresses $P_{12}(\dot{\gamma}_1)$ are 2.50×10^3, 4.78×10^3, and 5.94×10^3, respectively, and $P_{12}(\dot{\gamma}_2)$ is 8.28×10^3 dyn/cm^2.

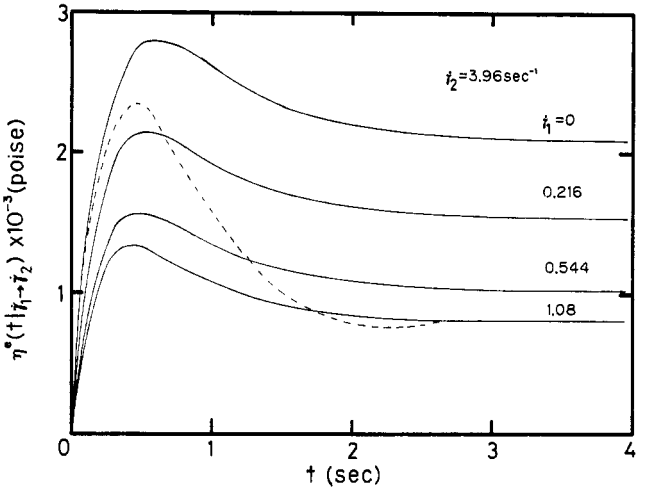

Figure 4. Experimental excess transient viscosity $\eta^e(t)$ evaluated from the data in Figure 3. The shear rates $\dot{\gamma}_1$ and $\dot{\gamma}_2$ are denoted in the figure. The broken line denotes calculated values of eq 6 using two experimental stress-development data from rest to $\dot{\gamma} = 1.08$ and 3.96 s^{-1}.

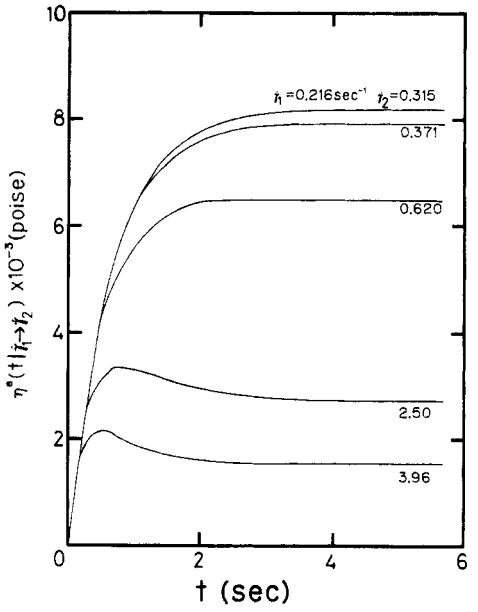

Figure 5. Experimental excess transient viscosity $\eta^e(t)$ in the experiments from a constant $\dot{\gamma}_1$ to various $\dot{\gamma}_2$ for the same samples as in Figure 1. The shear rates $\dot{\gamma}_1$ and $\dot{\gamma}_2$ are denoted in the figure.

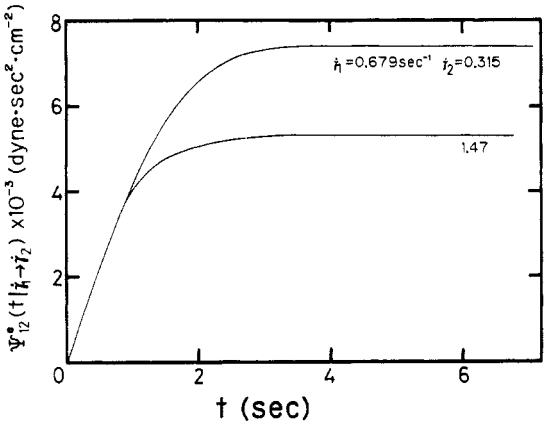

Figure 6. Experimental excess normal stress coefficient $\Psi_{12}^e(t)$ in the experiments from a constant $\dot{\gamma}_1$ to various $\dot{\gamma}_2$. Sample is an α-CN solution of F-288 (12.9 g/dL). The shear rates $\dot{\gamma}_1$ and $\dot{\gamma}_2$ are denoted in the figure.

same value of $\dot{\gamma}_2$ is also shown in this figure by a solid line. The maximum, i.e., the stress overshoot, can be clearly observed in the course of stress development. To examine the relationship of eq 6 in nonlinear regions, $\eta^e(t|\dot{\gamma}_1 \rightarrow \dot{\gamma}_2)$ in the experiments from various $\dot{\gamma}_1$ to a constant $\dot{\gamma}_2$ are shown by solid lines in Figure 4. The broken line denotes the calculated values of the right-hand side of eq 6 using two experimental stress development data in the onset of steady shear flows from rest to $\dot{\gamma}$ = 1.08 and 3.96 s^{-1}, respectively. The broken line corresponds to the lowest solid line in Figure 4. It is clear that eq 6 does not agree with the experimental $\eta^e(t|\dot{\gamma}_1 \rightarrow \dot{\gamma}_2)$ data in the nonlinear region. In particular, it should be pointed out that at the beginning of stress development the right-hand side of eq 6 gives the same slope as the experimental $\eta^e(t|\dot{\gamma}_1 \rightarrow \dot{\gamma}_2)$ data at the limit of $\dot{\gamma}_1 = 0$ rather than that at the experimental shear rate ($\dot{\gamma}_1$ = 1.08). It can also be pointed out that the initial slopes of solid lines are different with different $\dot{\gamma}_1$.

Examples of $\eta^e(t|\dot{\gamma}_1 \rightarrow \dot{\gamma}_2)$ and $\Psi_{12}^e(t|\dot{\gamma}_1 \rightarrow \dot{\gamma}_2)$ in the experiments from constant $\dot{\gamma}_1$ to various $\dot{\gamma}_2$ are shown in Figures 5 and 6, respectively. Examples of the stress development from rest ($\eta^d(t|\dot{\gamma})$ and $\Psi_{12}^d(t|\dot{\gamma})$) are shown in Figures 7 and 8, respectively. It can be seen in these figures that all curves increase from the origin with the same slope.

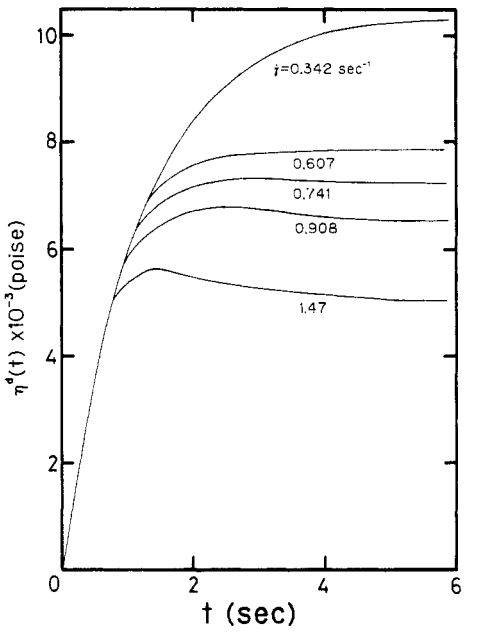

Figure 7. Experimental transient viscosity $\eta^d(t)$ after the onset of steady shear flow for the same samples as in Figure 6. The shear rates are denoted in the figure.

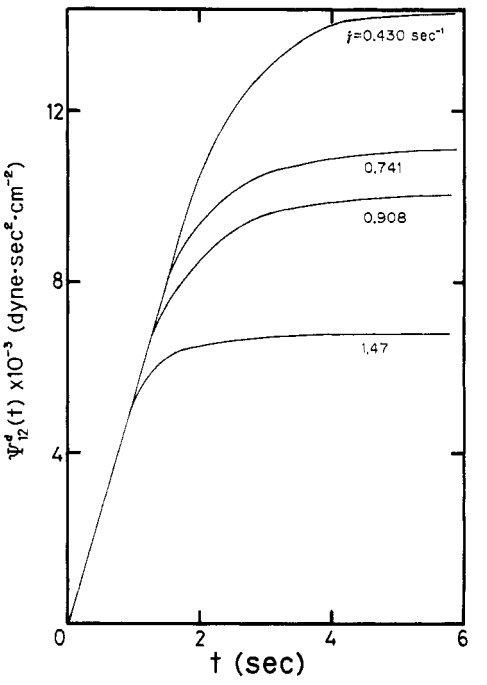

Figure 8. Experimental transient normal stress coefficient $\Psi_{12}^d(t)$ after the onset of steady shear flow for the same samples as in Figure 6. The shear rates are denoted in the figure.

It may be concluded that the original structure remains unchanged for a certain period t_c after the stepwise increases of shear rate not only from rest but also from finite values of $\dot{\gamma}_1$.

The time t_c, when the curves begin to deviate from the universal line, in the experiments at high $\dot{\gamma}_2$ can be roughly estimated in Figures 5–8. The critical strain γ_c, which is needed to start the rupture of the original quasi-network structure, may be given by $\gamma_c \equiv t_c(\dot{\gamma}_2 - \dot{\gamma}_1)$. The γ_c values estimated in the experiments from rest ($\dot{\gamma}_1 = 0$) are roughly $\gamma_c \simeq 1$ for all solutions used in this work. The value of γ_c in polymer–good solvent systems appears to be in the vicinity of unity, as pointed out by Menezes and Graessley[6,7] ($\gamma_c \simeq 1$ for polystyrene in tricresyl phosphate, $\simeq 0.9$

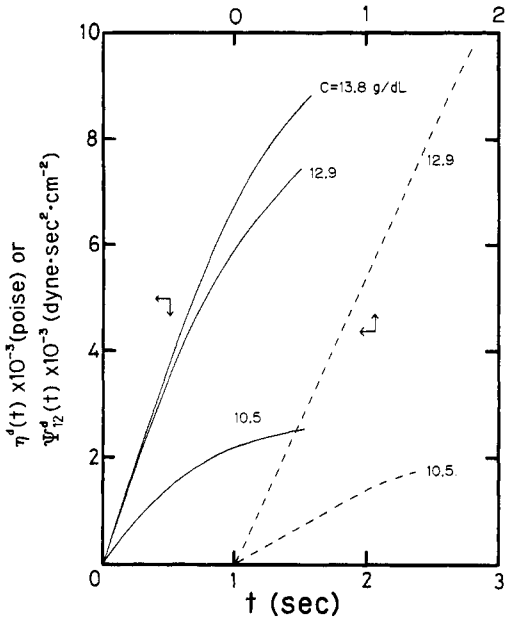

Figure 9. Initial parts of stress development observed after the onset of steady shear flow for all samples used in this work. The solid and broken lines denote $\eta^d(t)$ and $\Psi_{12}^d(t)$, respectively. Concentrations of sample solutions are denoted in the figure.

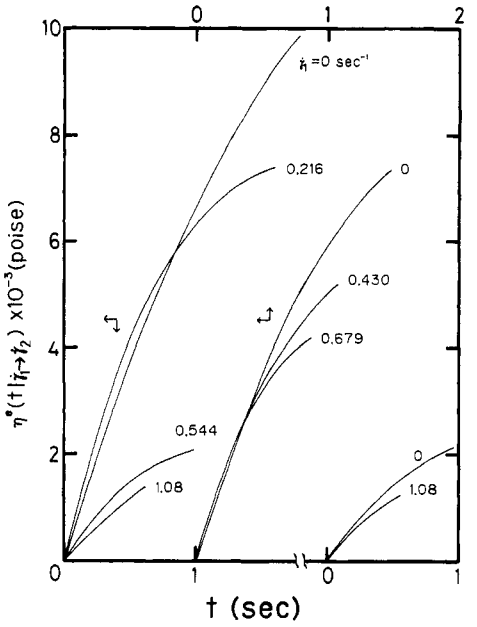

Figure 10. Initial parts of shear stress development observed after stepwise increase of shear rate from various $\dot{\gamma}_1$. Concentrations are 13.8, 12.9, and 10.5 g/dL from left to right. The shear rate $\dot{\gamma}_1$ is denoted in the figure.

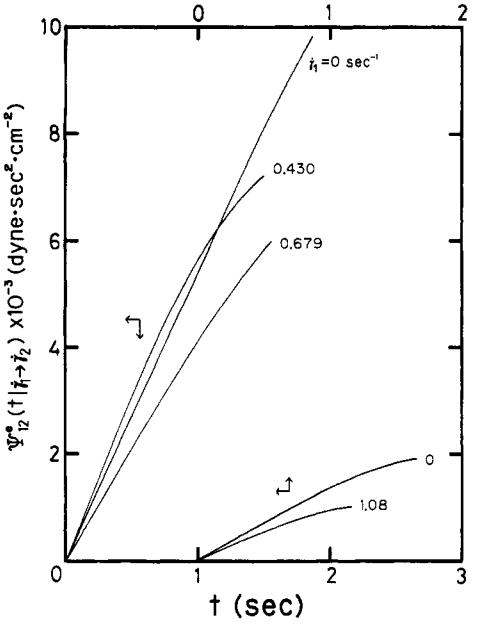

Figure 11. Initial parts of normal stress development from various $\dot{\gamma}_1$. Concentrations are 12.9 and 10.5 g/dL for left and right. The shear rate $\dot{\gamma}_1$ is denoted in the figure.

for polybutadiene in a commercial hydrocarbon oil (Flexon 391), and $\simeq 0.7$ for poly(α-methylstyrene) in diphenyl chloride).[4,5] The γ_c values in the transition from finite values of $\dot{\gamma}_1$ could not be estimated with high accuracy because of small values of t_c. At least, however, it was observed that γ_c is appreciably lower than unity. This low value is understandable if we take into account the difference between conformations of polymer chains at rest and under steady shear flow. Polymer chains under steady shear flow have stretched conformations.

Figures 3 and 5 show that the stress overshoot is observed not only in the stress development from rest but also in the stepwise increases of shear rate if the difference in entanglement density between two states is large. The peak position and its height may be determined by combination of the transfer or aftereffect function from the value at $\dot{\gamma}_1$ to that at $\dot{\gamma}_2$ and the stress development in the solution, but quantitative discussion cannot be given in this paper.

The entanglement density in polymer solutions can be changed by altering the polymer concentration. Any difference in the structure (entanglement density) of a polymer solution is reflected in the material function $\phi(t - t'|0)$ and, in turn, in the initial slope of stress development. The initial parts of $\eta^d(t)$ and $\Psi_{12}^d(t)$ at different concentrations are shown in Figure 9. The slope becomes lower with decreasing concentration, corresponding to a decrease in entanglement density. The initial slopes of shear and normal stress development curves from various values of $\dot{\gamma}_1$ are summarized in Figures 10 and 11, respectively. It can be observed that the slopes become lower with increasing $\dot{\gamma}_1$, though the slope appears to be somewhat enhanced when $\dot{\gamma}_1$ is only slightly outside the linear region. Comparisons among Figures 9–11 may support our speculation that the shear rate dependence of $\eta^e(t|\dot{\gamma}_1 \rightarrow \dot{\gamma}_2)$ or $\Psi_{12}^e(t|\dot{\gamma}_1 \rightarrow \dot{\gamma}_2)$ in the initial range is caused by the difference in the effective entanglement density at different $\dot{\gamma}_1$.

In this paper as well as in a previous paper,[4] we employed the aftereffect function expressed as a function of shear rate. The same stress development phenomena after onset of steady shear flow from rest to various values of shear rate were also discussed by Menezes and Graessley[7] using the modified Bernstein–Kearsley–Zapas theory[14] in which the memory function is defined as a function of strain. In their work, too, the experimental data could not be explained without assuming a time lag in the transition of the memory function from the linear form to nonlinear forms.

Thus, it may be concluded that the aftereffect function or the memory function in the constitutive equations should be defined corresponding to the structure of the material, as pointed out by Kajiura et al.[4] In general, however, the additivity of responses in viscoelastic behavior of polymer solutions does not hold in nonlinear regions.

Acknowledgment. This work was supported by a Grant-in-Aid for Scientific Research (No. 5675-0611) from

the Ministry of Education, Science, and Culture of Japan.

Registry No. Polystyrene, 9003-53-6.

References and Notes

(1) Sakai, M.; Fujimoto, T.; Nagasawa, M. *Macromolecules* **1972**, *5*, 786.
(2) Graessley, W. W. *Adv. Polym. Sci.* **1974**, *16*.
(3) Ferry, J. D. "Viscoelastic Properties of Polymers", 3rd ed.; New York, 1980.
(4) Kajiura, H.; Sakai, M.; Nagasawa, M. *Trans. Soc. Rheol.* **1974**, *18* (2), 323; **1976**, *20* (4), 575.
(5) Isono, Y.; Nagasawa, M. *Macromolecules* **1980**, *13*, 862.
(6) Menezes, E. V.; Graessley, W. W. *Rheol. Acta* **1980**, *19*, 38.
(7) Menezes, E. V.; Graessley, W. W. *J. Polym. Sci., Polym. Phys. Ed.* **1982**, *20*, 1817.
(8) Lodge, A. S. "Elastic Liquids"; Academic Press: London and New York, 1964.
(9) Yamamoto, M. "Buttai-no-Henkeigaku"; Seibundo & Shinkosha; Tokyo, 1972.
(10) Graessley, W. W.; Park, W. S.; Crawley, R. L. *Rheol. Acta* **1977**, *16*, 291.
(11) Endo, H.; Nagasawa, M. *J. Polym. Sci., Polym. Phys. Ed.* **1970**, *8*, 371.
(12) Sakai, M.; Fukaya, H.; Nagasawa, M. *Trans. Soc. Rheol.* **1972**, *16* (4), 635.
(13) Kajiura, H.; Endo, H.; Nagasawa, M. *J. Polym. Sci., Polym. Phys. Ed.* **1973**, *11*, 2371.
(14) Bernstein, B.; Kearsley, E. A.; Zapas, L. J. *Trans. Soc. Rheol.* **1963**, *7*, 391.

Distribution Functions for Gaussian Semilinear Polymers

Henryk Galina

Institute of Organic and Polymer Technology, Technical University, Wyb. Wyspiańskiego 27, 50-370 Wrocław, Poland. *Received July 29, 1985*

ABSTRACT: Distribution functions of the square radius of gyration have been calculated numerically for a class of Gaussian semilinear polymers consisting of branched or cyclic structural elements linked together by single bonds into a linear chain. In the calculations, only the characteristic polynomials of the Kirchhoff matrices of graphs representing these polymers were used. It has been shown that the first moments of the distribution, the mean square radii of gyration of the semilinear polymers, are readily obtainable directly from the analytically expressed characteristic polynomials. Purely graph-theoretical arguments have been used to determine the mean square radius of gyration for any sufficiently long semilinear molecule.

Introduction

Gaussian molecules provide a useful model for studying configurational behavior of real polymers. The disadvantages of the model, related to the approximations involved in it, are balanced, to some extent, by the relative simplicity of expressions describing various experimentally verifiable configurational properties of a polymer molecule.[1,2]

The calculations of the distribution functions of the square radius of gyration for Gaussian molecules of arbitrary connectivity becomes relatively easy when applying the graph–matrix method developed, principally, by Eichinger.[3–7] If the connectivity within a molecule follows a pattern of symmetry, the moments of the distribution can be expressed analytically,[4] and the calculation of the distribution function itself requires a simple numerical integration.[8] It has been done for linear,[9,10] comblike,[7,9] and ring[11] chains, as well as for star molecules[8,11] and regular nets.[8]

It has been shown[12,13] that for Gaussian cyclopolymers, too, the mean square radius of gyration can be calculated by merely inspecting the structure of the cycle-containing repeating elements of a polymer chain.

The dimensions of cycle-containing polymer molecules are of particular interest since it has been found that the size of cyclic molecules may affect the course of crosslinking in vinyl–divinyl polymerization.[14]

So far, two quite different estimates of the effect of cycles on dimensions of volumeless models of polymer molecules have been published.[15–18] The first, given by Allen et al.,[16] predicts a substantial collapse of randomly cyclized molecules, while the calculations by Martin and Eichinger[18] predict a much more moderate decrease in the dimensions of cyclic molecules compared with their linear analogues.

In fact, in the estimation by Martin and Eichinger,[18] the formation of small rings has been assigned a higher probability compared with formation of larger ones, and therefore this latter approach seems better suited for the cyclization occurring during polymer growth in vinyl–divinyl polymerization.

In this context, the cyclopolymerization constitutes the extreme case where only the smallest cycles are formed along essentially linear chains.

This paper deals with the evaluation of distribution functions of the square radius of gyration for a general class of Gaussian semilinear polymer molecules, including comblike and cyclopolymers. Numerically calculated distribution functions for such molecules differing in connectivity within repeating structural elements are compared.

Theoretical Background

Consider a molecule consisting of N beads connected pairwise with at least $N - 1$ identical springs. Assume[11,19] (i) the vector linking any two beads follows a Gaussian distribution (that is why the molecule is called the Gaussian), and (ii) the contribution of springs to the configurational potential is additive.

An instantaneous configuration of a molecule in a d-dimensional Cartesian system is fully described by the $d \times N$ matrix $\mathbf{R} = (\mathbf{r}_1, \mathbf{r}_2, ..., \mathbf{r}_N)$, where $\mathbf{r}_j$ is the vector linking the center of mass of the molecule with the jth bead.

The assumption (ii) implies the following form of the configurational potential of the molecule:[4,8]

$$V(R) = kT\gamma\sum_{i-j}(\mathbf{r}_i - \mathbf{r}_j)^2 = kT\gamma \text{ Tr } (\mathbf{RKR}^T) \qquad (1)$$

while the assumption (i) imposes the condition $\gamma = d/2\langle l^2\rangle_0$, where $\langle l^2\rangle_0$ is the mean square spring extension. The summation in eq 1 runs over all springs directly

0024-9297/86/2219-1222$01.50/0